Desalination and Water Treatment
www.deswater.com

1944-3994/1944-3986 © 2012 Desalination Publications. All rights reserved
doi: 10/5004/dwt.2012.1509

Taylor & Francis
Taylor & Francis Group

40 (2012) 1–6
February

Nanotechnology: the next revolution for wastewater treatment (TNT contaminate)

Abdelfattah Mohsen Badawi[a], Sahar Mustafa Ahmed[a], Seham Ali Shaban[a,*], Salwa Mohamed Ibrahim Morsy[a,b]

[a]*Egyptian Petroleum Research Institute Nasr City, Cairo, Egypt*
Tel. +2 222745902; Fax: +20 222745902; email: sehamshaban@yahoo.com
[b]*Chemistry Department, Faculty of Science, Taif University, Kingdom of Saudi Arabia*

Received 27 June 2011; Accepted 18 October 2011

ABSTRACT

Trinitrotoluene (TNT), a nitroaromatic explosive, is encountered groundwater contaminant that can pose a human health risk, even at very low aqueous concentrations. In this study, a series of catalytic degradation of dissolved TNT have been investigated using iron nanocatalysts (zero valent and its oxide) and Fe_2O_3 bentonite nanocomposite. The prepared nano catalysts were characterized via XRD, BET and TEM. The degradation of TNT by Fe-PILC, is almost complete after 30 min, whereas 65, 100 min on using the Fe-zero valent and Fe-oxide, respectively. These results indicate that the reaction rate is a strong function of the number of iron surface active sites, and therefore the Fe-catalysts an important reaction variable.

Keywords: Trinitrotoluene (TNT); Nanotechnology; Catalytic degradation wastewater; Fe_2O_3 bentonite nanocomposite; Fe-zero valent; Fe-oxide; Iron nanocatalysts

---

1. Introduction

2,4,6-Trinitrotoluene (TNT) has been the most widely used nitroaromatic explosive and TNT concentrations have been reported to range from 10 to 12,000 mg kg^{-1} at contaminated sites [1]. Most of these sites contain also contaminated groundwater.

Nanocatalysts have the advantage of very high reaction rates due to high specific surface areas and low mass-transfer restrictions. These nano-catalysts have been successfully tested in different reactor systems at the laboratory scale [2]. Zero valent iron treatments have been successfully applied for TNT degradation in water and soil treatment [3], Fenton-like reactions using iron minerals as heterogeneous catalysts is scarcely available [4], although the efficiency of such processes has been clearly demonstrated for others organic pollutants [5,6]. Heterogeneous catalysis offers significant advantages. Use of iron oxides instead of dissolved iron may be especially advantageous for in situ remediation of contaminated groundwater where pH cannot be adjusted. The catalyst can be easily recovered by sedimentation or filtration for further uses.

In this paper, the synthesis of nanocomposite bentonite clay based Fe, zero-valent iron nanocatalysts and its oxide was performed. The catalytic activity of the prepared nano catalysts for TNT degradation was evaluated in aqueous solution.

---

*Corresponding author.

2. Experimental

2.1. Instruments

1. X-ray diffraction was carried out for the catalyst samples, with a Philips diffractometer (type pw1050) at $\lambda = 1.54$ Å. A Cu Kα target with a nickel filter.
2. Surface area and pore volume of catalyst samples were analyzed by means of nitrogen adsorption using Nova 2000, Quanta Chrome (commercial BET unit).
3. TEM image and selected-area electron diffraction (SAED) was taken with a JEOL JEM-2000 EX model transmission electron microscope, using an accelerating voltage of 100 kV. The sample of TEM was prepared by 2 h ultrasonic dispersion of 0.2 g of product in 50 ml ethanol. Then, a drop of the solution was placed on a copper micro grid, and dried in air before performance.
4. High performance liquid chromatography (HPLC)

   Apparatus: HPLC Waters 600 Equipped with: an autosampler (Waters 717 plus) and a dual wavelength absorbance diode array detector (Waters 4487) set at 254 nm.

   Column: C 18 column for TNT column length: 15 cm, internal diameter: 46 mm. The mobile phase: grade water/acetonitrile (40/60) operating at a flow rate of 1 cm^3 min^{-1}.

2.2. Synthesis of nanocatalysts

2.2.1. Synthesis of iron nanocatalysts (zero valent and its oxide) by reduction with hydrazine hydrate

A clear iron solution in ethylene glycol was prepared by dissolving a certain amount of iron salt ($FeSO_4$) in 50 ml of ethylene glycol. Heating at 90°C attained complete solubility of the salt. The iron metal was obtained from the prepared solutions by adding a different amounts of hydrazine hydrate ($N_2H_2 \cdot H_2O$) solution (80 vol%) drop wisely to the previously prepared solution of iron salt in ethylene glycol under constant stirring. The addition of hydrazine resulted in changing the color of solution from blue to brown-reddish brown. After about 10 min, sodium hydroxide solution was added till pH of the solution is reached 11–12 after which a black solid precipitate of iron metal zero valent was precipitated. The obtained iron zero valent was collected after washing several times with organic solvent (acetone or alcohol). Ferric oxide was obtained by calcined of iron zero valent at 400°C for 2 h [7].

2.2.2. Synthesis of Fe_2O_3 bentonite nanocomposite (Fe-PILC)

A solution of 0.2 M ferric nitrate was prepared by dissolving the equivalent amount of the salt in deionized and distilled water. Solid sodium carbonate was added slowly to alter the pH of the solution. Hydrolysis of ferric nitrate with sodium carbonate was carried out at 25°C, and an aging period of 24 h was allowed as suggested by Saeedeh [8]. The value of OH/Fe was 2.0 and the pH of this solution was 1.8. A suspension containing 1.0 g of bentonite clay in 100 ml water was added to the hydrolyzed ferric solution. This suspension and the pillaring agent were vigorously stirred at room temperature for 24 h, recovered by filtration, washed repeatedly with water, and then dried in air overnight at 110°C. The filtrate was calcined at 300°C for 5 h. The relevant physical and chemical properties of the nanocatalysts are presented in Table 1. Nanocatalysts with a wide range of particle sizes and specific surface areas were evaluated.

2.3. Chemicals and batch reactor

Experiments were performed using (0.044%) TNT explosives dissolved in distilled water. Solutions at three different pH levels (4, 7, and 10) were placed in a flask containing accurately weighed amounts of the different nanocatalyst samples. Constant pH levels were maintained during the batch experiments at room temperature using pH controller that dispensed concentration of 0.27 HCl and 0.25 NaOH solutions into the reactor. The nanocatalyst samples weight around 0.3 g l^{-1} of solutions. The flasks were shaken at 200 rpm using an electric shaker for a prescribed length of time to attain equilibrium. After filtration, TNT analyses were performed using HPLC [9].

2.4. Photocatalytic decomposition of TNT

The experiments were carried out in a photocatalytic reactor in the center of the cylindrical reactor, using a 50 W, tungsten–halogen lamp (400–800 nm). The decay of TNT in aqueous medium was evaluated at different irradiation periods. Prior to starting illumination, a suspension containing 0.3 g l^{-1} of catalyst and 0.1 g l^{-1} of TNT were stirred continuously in the dark for 15 min. The concentration of TNT in solution at this point was used as the initial value for the kinetic treatment of the photodegradation processes. Cooling by water circulation

Table 1
Physico-chemical characteristics of prepared catalysts

Sample	Surface area, m^2 g^{-1}	Particle size, nm
Fe-PILC	280	12.2
Fe-zero valent	214	9.9
Fe-oxide	150	5.2

at 25°C during the experiments was performed at constant stirring at given intervals of illumination, a sample of the catalysts particulate was collected, centrifuged, After filtration TNT analyses were performed using HPLC. The concentrations of TNT in the aqueous samples were measured according to Standard Method for the trace analysis of explosive residues by HPLC using a UV detector. Calibration of the HPLC was performed using external standards with concentrations ranging from 0 to 100 mg l^{-1} using serial dilution of the stock solutions.

3. Result and discussion

3.1. Characterization of Fe-nanocatalysts

3.1.1. X-ray diffraction (XRD)

The products were firstly checked by XRD technique to learn their phase compositions. The XRD pattern (Fe-PILC) shows diffraction peaks at 2θ = 26.6° and 19.88° (Fig. 1(a)), which are assigned to SiO_2 crystallite [10]. For Fe-PILC, the main diffraction peaks are at 2θ = 33.1° and 35.6°, assigned to Fe_2O_3 crystals. These indicated that Fe particle are intercalated in silicate layers in the catalysts.

Fig. 1(b) is represented the XRD pattern of Fe-zero valent. The reflection peaks at 2θ = 19.3°, 27.5° and 33.8° and 54.8° correspond to the characteristic inter planar spacing between (1 1 0), (2 0 0), (2 1 1) and (3 2 1) planes of Fe-zero valent. While Fig. 1(c) shows that Fe-oxide, peaks centered at 2θ = 30.1°, 33.1°, 35.6° and 49.4° can be indexed to the reflections of (1 0 4), (1 1 0), (0 2 4) and (1 1 6) planes of Fe-oxide [11]. The size particles calculated from these data for the current catalysts are listed in Table 1.

3.1.2. Textural characteristics

The surface texture properties of the samples have been assessed from nitrogen adsorption isotherms at 196°C. All the samples displayed type II (Fig. 2) in the IUPAC classification [12]. The Fe-zero valent have a surface area of 214 $m^2 g^{-1}$ while Fe-oxide particles have a surface area of 150 $m^2 g^{-1}$ measured by Brunauer, Emmett and Teller (BET) adsorption isotherms [13]. Evidently, the combined Fe pillaring has increased the surface area than that of the Fe-oxide or Fe-zero valent (Table 1) [14].

3.1.3. Transmission electron microscopy (TEM)

Morphology of composite membranes For the purpose of clarifying the size of nano iron in the composite membrane, the TEM images were made as shown in Fig. 3. It can be seen that less than 50 nm diameters of iron particles can be found in this TEM image.

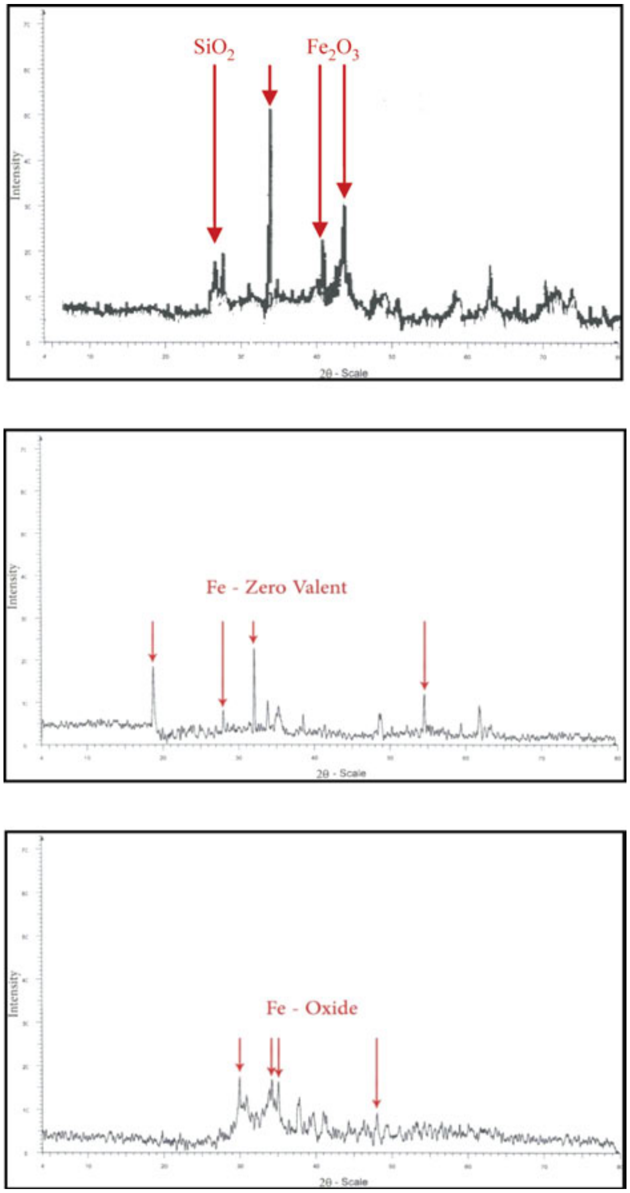

Fig. 1. XRD pattern of (a) Fe-PILC, (b) Fe-zero valent and (c) Fe-oxide.

The results indicated that iron can be present in nanosize membranes. Similar results were also found in recent years [15,16].

3.2. TNT degradation at different pH values

Fig. 4 shows the aqueous concentrations of TNT during transformation by Fe-PILC in solutions with different pH. At pH 4.7, TNT was rapidly removed from solution: 98.9% of the initial TNT disappeared after 10 min. Transformation of TNT at pH 7.4 and pH 9.7 was substantially slower. At pH 7.4 complete removal of TNT was observed

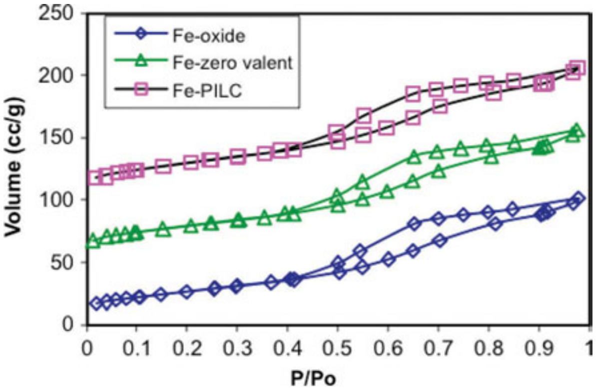

Fig. 2. Textural characteristics of (a) Fe-PILC, (b) Fe-zero valent and (c) Fe-oxide.

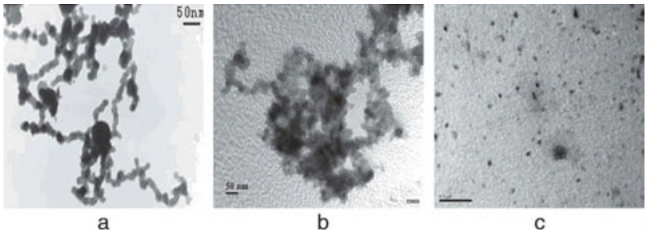

Fig. 3. TEM image of nano catalysts. (a) Fe-PILC, (b) Fe-zero valent and (c) Fe oxide.

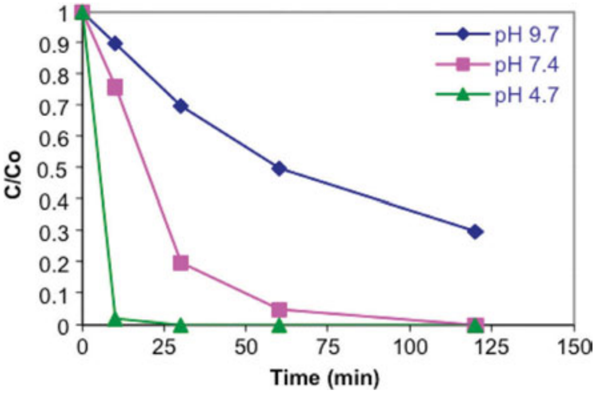

Fig. 4. TNT degradation by Fe-PILC with different pH.

within 120 min, whereas 27% of TNT still remained in solution after 120 min at pH 9.7. These results indicate that solution pH has a strong effect on the reduction kinetics of TNT. Accelerated iron corrosion under acidic conditions may be responsible for the enhanced reduction. Therefore, optimum initial pH values of Fe-PILC solution was chosen to be 4.7, and we can apply optimum pH values on other nanocatalysts samples.

3.3. Treatment of TNT using Fe-PILC, Fe-zero valent and Fe-oxide nanoscale

The effect of the contact time on the treatment of TNT is shown in Fig. 5. Fig. 5 compares the degradation of TNT in presence of the Fe-PILC, Fe-zero valent and Fe-oxide. The superiority of the former Fe-PILC catalyst is evident. Using the Fe-PILC, TNT degradation is almost complete after 30 min. However, on using Fe-zero valent and Fe-oxide the complete degradation was observed at 65 and 120 min, respectively. The higher activity of Fe-PILC can be attributed to its higher surface area.

TNT degradation experiments were carried out by varying the initial TNT concentration from 5.5 to 32.5 mg l^{-1} by using Fe-PILC, Fe-zero valent and Fe-oxide as nanocatalyst. Fig. 6 shows the degradation of TNT decreased by increasing the TNT concentration.

Experimental data and the curve for TNT degradation are shown in Fig. 6 indicate that the highest degradation value corresponds to the lowest initial TNT concentration (5.5 mg l^{-1}) and the lowest degradation value corresponds to the highest initial TNT concentration (32.5 mg l^{-1}). These results indicate that the reaction rate is a strong function of the number of iron surface active sites, and therefore the Fe-catalyst: TNT molar ratio is an important reaction variable.

3.4. Photocatalytic degradation of TNT on Fe-PILC

The evaluation of Fe-PILC catalyst was conducted in a batch photoreactor using a halogen lamp inserted in the center of the reactor and surrounded by a quartz cooling jacket.

Hydrogen peroxide was used in the present work according to advanced oxidation technology (AOT) for activating the photocatalytic degradation using the prepared Fe-PILC nonocomposite catalyst. Fig. 7 depicts the TNT degradation activity of this catalyst in presence

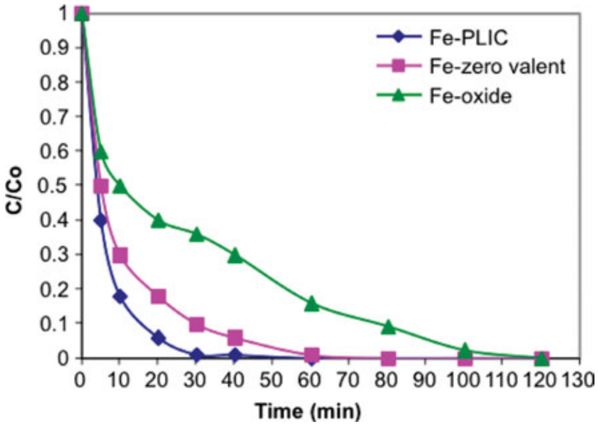

Fig. 5. Degradation of TNT using Fe-PILC, Fe-zero valent and Fe-oxide as nanocatalysts.

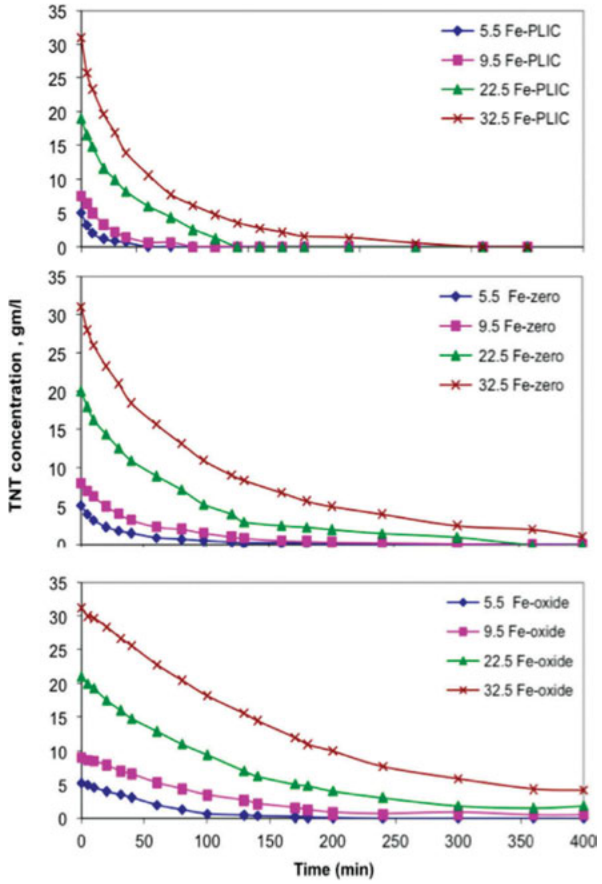

Fig. 6. Time concentration profile for TNT reduction at various initial concentrations and fixed initial amount of Fe-nanocatalysts. Initial TNT (mg l^{-1}): 5.5, 9.5, 22.5, 32.5.

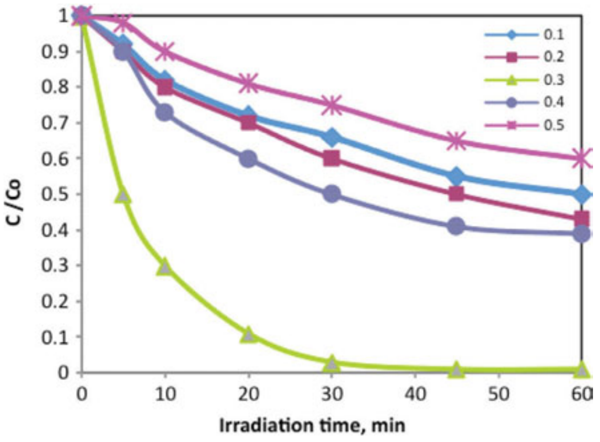

Fig. 7. Effect of H_2O_2 on the degradation of TNT.

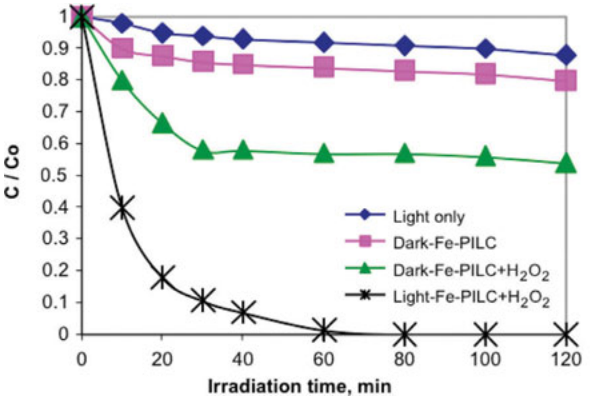

Fig. 8. Photocatalytic degradation of TNT using Fe-PILC at (pH = 7.0).

of H_2O_2. Hence, in this work, the optimum concentration of H_2O_2 (0.3 m mol^{-1}) was always used. This phenomenon has been attributed [17] to the favorable role of hydrogen peroxide to continue the oxidation of the reaction products and avoiding their re-adsorption on the catalyst surface which, at higher concentration of H_2O_2, can compete with the TNT for adsorption sites on the surface. The degradation process takes place by combination of adsorption process of the TNT on the surface of nano-composite catalyst which causes the degradation of TNT and the photo-oxidation process of the TNT by oxidizing species.

Irradiation of an aqueous solution containing a TNT with visible light in absence of a catalyst has been carried out for incremental periods up to 120 min, where 16.0% degradation took place Fig. 8. The experiment was again carried out in dark but in presence of the Fe-PILC to examine the behavior of adsorption of TNT on the surface of this clay. It is found that during the initial 5 min, 10.0% degradation of TNT took place, Fig. 8 beyond which the desorption rate took place more slowly till at 120 min 25% degradation was achieved. Repeating this experiment, also in dark and in presence of the same quantity of Fe-PILC, but, moreover adding 0.3 m mol l^{-1} of H_2O_2, a more effective degradation was achieved, such that during the initial 5 min, as high as 19.8% of TNT degradation, and after 20 min 49.5% degradation. Nevertheless, at 20 min, degradation amounted to 49.5%. Beyond 20 min, degradation became insignificant such that it comprised 55.0% at 120 min. This experiment shows how effective has been the addition of H_2O_2, although in dark. While using the Fe-PILC, TNT degradation is 97% after 30 min irradiation.

4. Conclusions

Increase importance is falling on technologies that can treat TNT pollution sites. With technologies such as adsorption and advanced oxidation processes.

The data indicated that Fe-bentonite nanocomposite due to its increased surface area than Fe-oxide or Fe-zero valent provide to be more effective for degradation of TNT contaminated wastewater.

Addition of 0.30 m mol l^{-1} of H_2O_2 is the optimum quantity found to be the most efficient for the photodgradation of TNT in aqueous solution. On using the Fe-PILC, TNT degradation is 97% after 30 min irradiation.

Acknowledgements

It is indebted to present our thanks for Egyptian Petroleum Research Institute (EPRI) and Ministry of Military Production—Center of Scientific Excellence who presented finance support of this research and covered the expense of all measurements.

References

[1] J. Rodgers and N. Bunce, Treatment methods for the removal of nitroaromatic explosives. Water Res., 35 (2001) 2101–2111.

[2] H. Hildebrand, K. Mackenzie and F.-D. Kopinke, Novel nanocatalysts for wastewater treatment, Global Nest J., 1(10) (2008) 47–53.

[3] J.Z. Bandstra, R. Miehr, R. Johnson and P. Tratnyek, Reduction of 2,4,6-trinitrotoluene by iron metal: kinetic controls on product distributions in batch experiments, Environ. Sci. Technol., 39 (2005) 230–238.

[4] T.F. Hess and P.S. Scharder, Coupled abiotic–biotic mineralization of 2,4,6-trinitrotoluene (TNT), J. Environ. Qual., 3 (2002) 736–744.

[5] H.H. Huang, M.C. Lu and J.N. Chen, Catalytic decomposition of hydrogen peroxide and 2-chlorophenol with iron oxides, Water Res., 35 (2001) 2291–2299.

[6] W.P. Kwan and B.M. Voelker, Influence of electrostatics on the oxidation rates of organic compounds in heterogeneous Fenton systems, Environ. Sci. Technol., 38 (2004) 3425–3481.

[7] S.M.I. Morsy, S.A. Shaban, A.M. Ibrahime and M.M. Selim, Characterization of cobalt oxide nanocatalysts prepared by microemulsion with different surfactants, reduction by hydrazine and mechanochemical method, J. Alloys Compd., 486 (2009) 83–87.

[8] H. Saeedeh, $MnFe_2O_4$/bentonite nano composite as a novel magnetic material for adsorption of acid red 138, Afr. J. Biotechnol., 9(50) 13 Dec. (2010) 8667–8671.

[9] M.E. Fuller, P.B. Hatzinger, D. Rungkamol, R.L. Schuster and R.J. Steffan, Enhancing the attenuation of explosives in surface soils at military facilities: combined sorption and biodegradation, Environ. Toxicol. Chem., 23 (2004) 313–324.

[10] J. Feng, X. Hu and P.L. Yue, Novel bentonite clay-based Fe-nanocomposite as a heterogeneous catalyst for photo-Fenton discoloration and mineralization of Orange II, Environ. Sci. Technol., 38 (2004) 269–275.

[11] A. Ghauch, A. Tuqan, and H. Abou Assi, Antibiotic removal from water: elimination of amoxicillin and ampicillin by microscale and nanoscale iron particles, Environ. Pollut., (5) (2009) 1626–1635.

[12] K.S.W. Sing, D.H. Everett, R.A.W. Haul, L. Moscou, R.A. Pierotti, J. Rouquerol and T. Siemieniewska, Pure Appl. Chem. 57(4) (1985) 603.

[13] M. Thommes, R. Koehn and M. Froeba, Sorption and pore condensation behavior of nitrogen, argon and krypton in mesoporous MCM-48 silica materials, J. Phys. Chem. B, 9 104 (33) (2000) 7932–7943.

[14] K.S. Lin, N.B. Chang and T.D. Chuang, Fine structure characterization of zero-valent iron nanoparticles for decontamination of nitrites and nitrates in wastewater and groundwater, Sci. Technol. Adv. Mater., 9 (2008).

[15] S.H. Chena, R.M. Lioua, C.L. Laia, M.Y. Hunga, M.H. Tsaib and S.L. Huangb, Embedded nano-iron polysulfone membrane for dehydration of the ethanol/water mixtures by pervaporation, Desalination, 234 (2008) 221–231.

[16] T. Yu, J. Lin, J. Xu, T. Chen and S. Lin, Novel polyacrylonitrile nanocomposites containing Na-montmorillonite and nano SiO_2 particle, Polymer, 46 (2005) 5695–5697.

[17] E.G. Garrido-Ramírez, K.G. Theng and M.L. Mora, Clays and oxide minerals as catalysts and nanocatalysts in Fenton-like reactions: a review, Appl. Clay Sci., 47(3–4) (2010) 182–192.